

DEFORMATION INTERACTION OF RC COLUMNS SUBJECTED TO TWO-DIMENSIONAL LATERAL LOADING

M. YOSHIMURA and K. TSUMURA

Department of Architecture, Faculty of Engineering, Tokyo Metropolitan University,
Minamiosawa 1-1, Hachioji, Tokyo, 192-03, Japan

ABSTRACT

Two-dimensional lateral loading tests of RC columns were conducted in such manner that they were cyclically loaded to one lateral direction under constant loads for the axial and other lateral directions. Observed relation between two lateral and axial deformation was studied. The study has revealed the flow rule in plasticity applies to RC columns for the interaction between these deformation on some condition. The test results were also simulated by the analytical model assuming the flow rule, and validity and limitations of the model were examined.

KEYWORDS

RC column; two-dimensional lateral loading; deformation interaction; yield surface; flow rule; plasticity.

INTRODUCTION

Damage to RC structures during severe earthquakes has demonstrated experimental and analytical research into the behavior of RC columns subjected to two-dimensional lateral loading is an urgent issue. Past efforts on this issue, mainly directed toward the interaction between two lateral loads, have revealed that the yield surface of flexural columns could be represented by a circle. However, the interaction between two lateral deformation, such as the direction of deformation increment when the load point is on the yield surface, has not been studied before. Thus, it was intended in this paper to observe and examine the deformation interaction of RC columns subjected to two-dimensional lateral loading.

TESTS

Specimens and Loading

Four identical specimens with 40 x 40 cm square section (Fig.1) designed to fail in flexure were fabricated. Yield stresses of main and lateral reinforcement were 375 and 347 Mpa, and compressive strength (σ_B) of concrete was 25.2 Mpa. Test parameters were the amplitude of jack load (N) for axial direction and that (PY_o) for one lateral (Y) direction: the former was set as a value corresponding to axial stress (σ_0) over σ_B of 0.2 or 0.4, and the latter was as about 1/5 or 2/5 of the yield load computed for one lateral direction (Table 1). The numerals after alphabet S in the specimen name denote the amplitude of the two parameters.

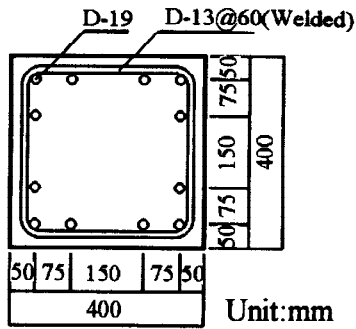


Fig.1 Section of specimen

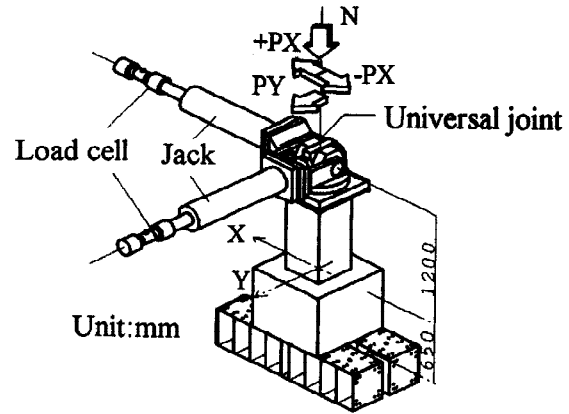


Fig.2 Loading apparatus

Table 1 Test parameters

Name	N [KN]	PY ₀ [KN]
S205	785(0.2) * ¹	49(5) * ²
S405	1570(0.4)	49(5)
S210	785(0.2)	98(10)
S410	1570(0.4)	98(10)

*1: σ_0 / σ_B

*2: in tonf

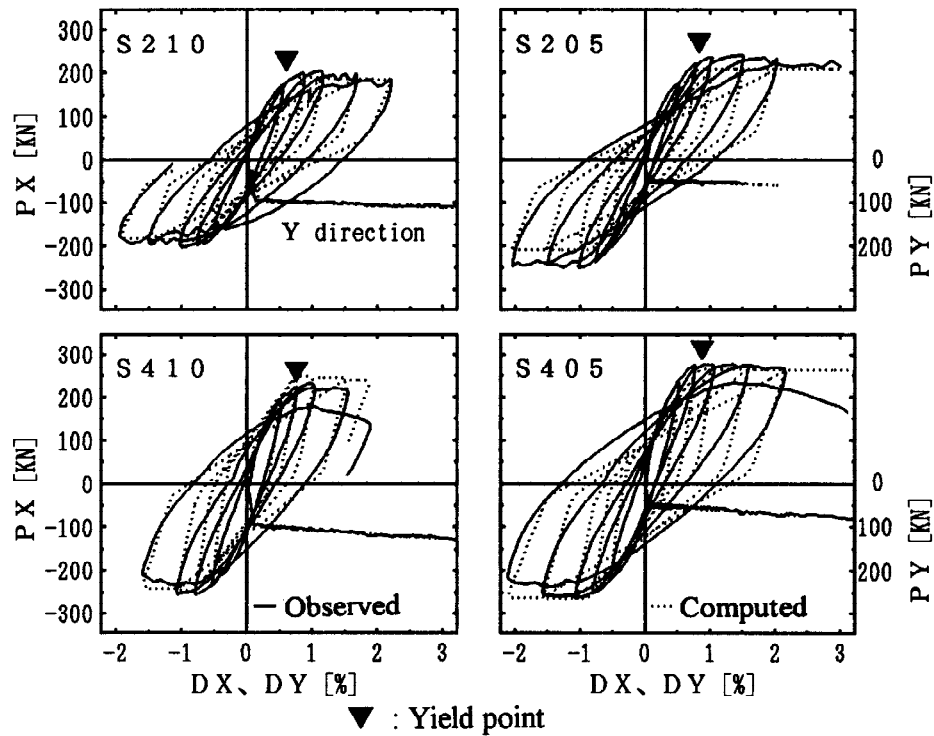


Fig.3 Lateral load vs. deflection relation

Loading apparatus is shown in Fig.2. The above two loads were first applied and were kept constant to a prescribed value. Loading for the other lateral (X) direction was then conducted in complete reversals. Actual lateral load on the laterally deformed condition differs from the jack load because of the effect of axial and other lateral load, or P- δ effect. Lateral load was, therefore, evaluated by modifying the jack load considering the P- δ effect.

Test Results

Lateral load and deflection for the X direction are referred to as PX and DX, and those for the Y direction as PY and DY. Lateral load vs. deflection relation is shown in Fig.3 by a solid line. The P- δ effect made PY gradually increase over PY₀. The point where more than three main bars yielded, was defined as a yield point and illustrated by symbol ▼ in the PX vs. DX relation. In the case of the same axial load, PX at the yield point was smaller for greater PY₀. (S210 < S205, S410 < S405), indicating the state of strength interaction. Note strength deterioration was observed in the case of high axial load (S410 and S405), which was more pronounced for greater PY₀.

DX vs. DY relation is shown in Fig.4. Despite PY₀ being constant throughout the test, DY was increasing as the loading proceeded, and the rate of DY's increase was: ① larger for greater PY₀ in the case of the same axial load (S210 > S205, S410 > S405), and ② close for different axial loads in the case of the same PY₀. (S210 \approx S410, S205 \approx S405) except for later loading cycles (after the 4th cycle) where strength deterioration occurred for S410 and S405. It should be noted DY was increasing substantially at DX being large during the loading of each cycle. PX vs. DY relation is shown in Fig.5. DY drastically increased near PX at the yield point, in other words, when the load point reached the yield surface, while it hardly increased on the other occasions. Note during the last loading cycle of S410 and S405, the DY's drastic increase occurred at a load

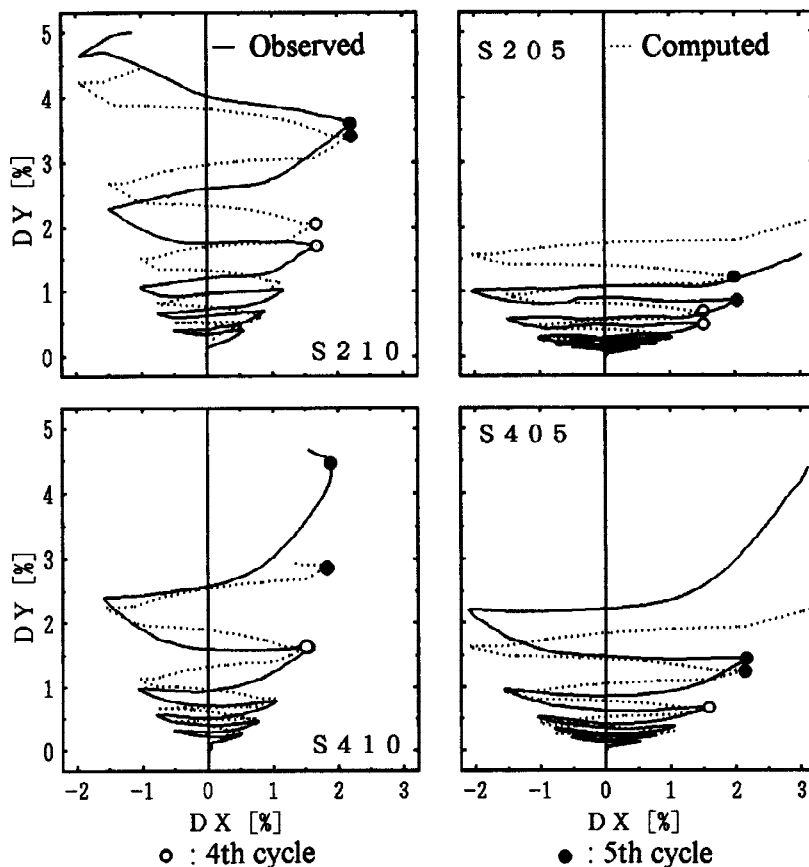


Fig.4 DX vs. DY relation

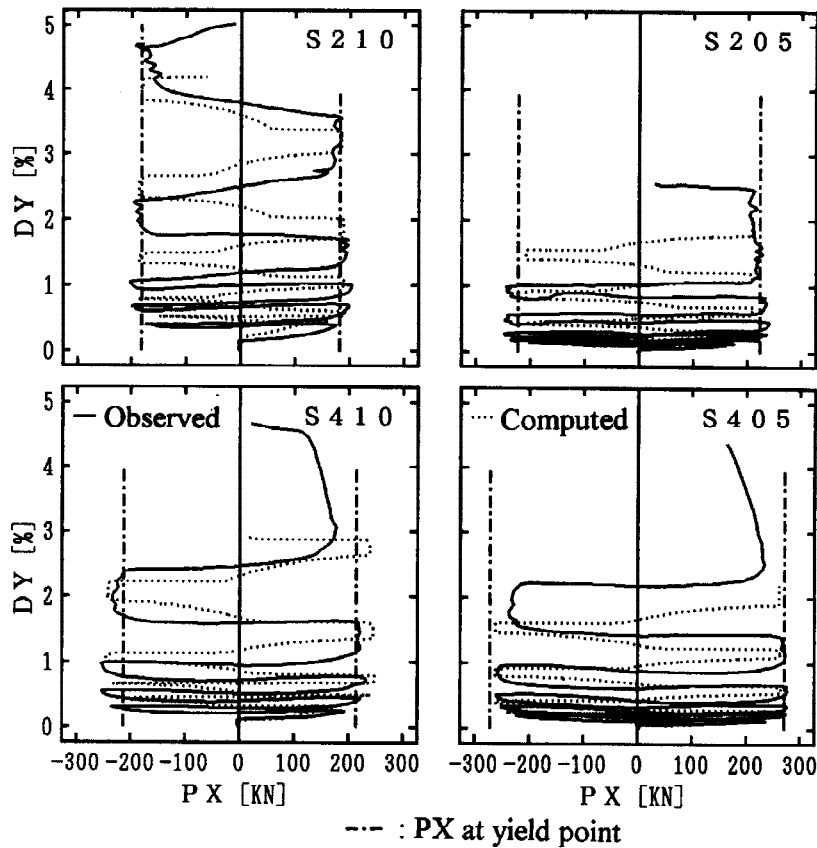


Fig.5 PX vs. DY relation

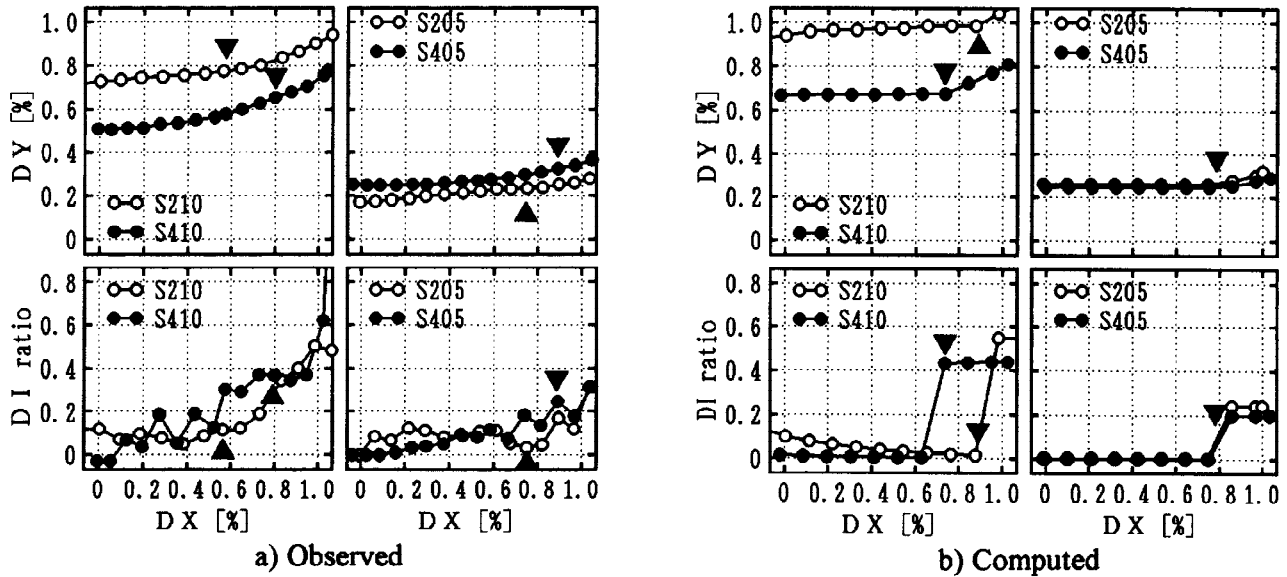


Fig.6 DX vs. DY and DX vs. DI ratio relation (Third cycle)

less than PX at the yield point because of the strength deterioration.

For the third cycle where the load point reached the yield surface for all specimens, DX vs. DY relation and relation between DX and the ratio (DI ratio) of DY's increment to DX's increment at each load step are plotted in Fig.6.a, where the DI ratio expresses tangential slope for the DX vs. DY relation. Symbol \blacktriangledown in the figure denotes the yield point. DY began increasing in the vicinity of the yield point for any specimen, and the DI ratio after this point ranged approximately from 0.2 to 0.6 for S210 and S410, and from 0.1 to 0.3 for S205 and S405: like the rate of DY's increase previously stated, the DI ratio was larger for greater P_{Y_0} ($S210 > S205$, $S410 > S405$) and close for different axial loads ($S210 \approx S410$, $S205 \approx S405$).

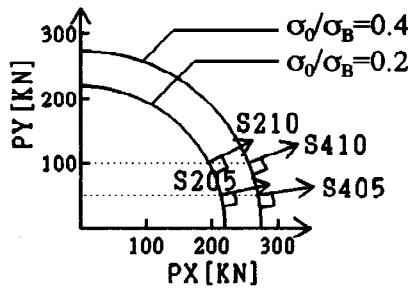


Fig. 7 Direction normal to PX-PY yield surface

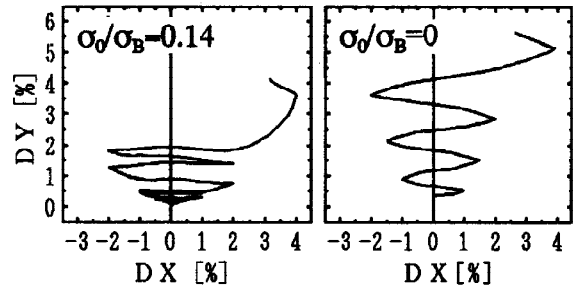


Fig. 8 DX vs. DY relation (different σ_o/σ_B)

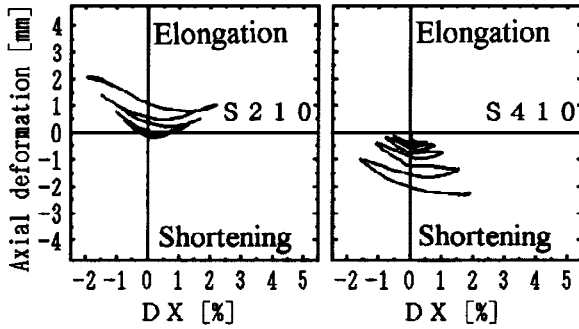


Fig. 9 DX vs. axial deformation relation

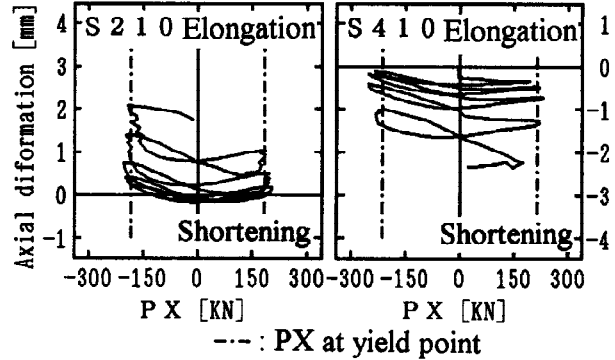


Fig. 10 PX vs. axial deformation relation

These results on DY's increase are herein discussed from the viewpoint of plasticity. It is assumed in the plasticity that when the load point reaches the yield surface, plastic flow occurs, the vector of which is directed along the normal to the yield surface, or flow rule. The normal to the yield surface is shown in Fig. 7 by an arrow for each specimen, where the yield surface was assumed as a circle and yield load for one direction was computed using a conventional equation. It is apparent that the direction of the arrows is consistent with the results on the DI ratio, indicating the flow rule applies to RC columns for the interaction between two lateral deformation.

The tests presented covered only two levels of axial stress: σ_o/σ_B of 0.2 and 0.4. It was, therefore, attempted to examine if the flow rule holds true for other levels of axial stress. The authors had before conducted other tests using the same loading method as employed here, where σ_o/σ_B was set as 0.14 and zero. DX vs. DY relation from these tests are shown in Fig. 8. With $\sigma_o/\sigma_B=0.14$ (Tsumura *et al.*, 1994), DY increased only at DX being large during the loading of each cycle like the results shown in Fig. 4. However, without axial load (Sato *et al.*, 1994), DY did not show such response but increased with a rather constant rate throughout the loading and unloading. The latter result was probably due to that without axial load, crack opening during the unloading may also be a source of the DY' increase as well as bar yielding during the loading. Anyhow, it is concluded for the interaction between two lateral deformation that the flow rule holds true so long as axial compression is applied.

The interaction between DX and axial deformation is discussed next. DX vs. axial deformation relation (Fig. 9) indicated axial elongation occurring for S210 and axial shortening for S210. And PX vs. axial deformation relation (Fig. 10) indicated that for S210 significant axial elongation occurred near PX at the yield point while for S410 axial shortening did not occur at all in this vicinity. One may consider these results are consistent with the flow rule on the DX vs. axial deformation relation: the direction of the normal to the PX vs. axial load yield surface indicates axial elongation for S210 and almost no axial deformation for S410 (Fig. 11). However, the fact of S410 that the shortening did not occur at the state of yielding but occurred on other occasions, does not seem to support the flow rule. It is, therefore, concluded for the interaction between lateral and axial deformation that the flow rule holds true only if axial compression is small enough to produce axial elongation. Note that Fig. 11 implies with respect to this matter the flow rule is likely to hold true if σ_o/σ_B is higher than 0.4, for which axial shortening is expected to occur.

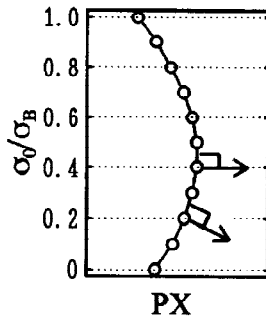


Fig. 11 Direction normal to PX-axial load yield surface

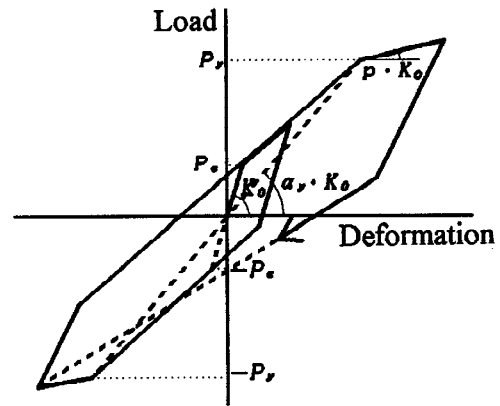
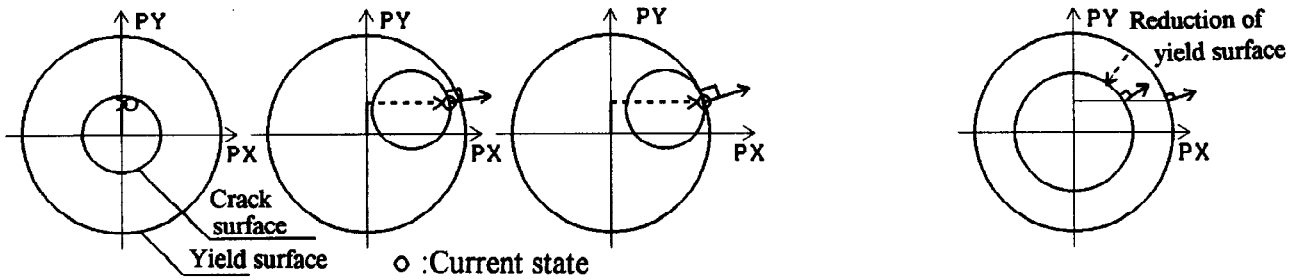


Fig. 12 Degrading Tri-Linear model (one lateral direction)



① Elastic range ② Crack range ③ Yield range
Fig. 13 Changes of range and direction of normal to surface

Fig. 14 Effect of reduction of yield surface

Table 2 Structural properties (one lateral direction)

Name	K_0 [KN/cm]	P_c [KN]	P_y [KN]	α_y	p
S205	804	74.9	215	0.274	0.001
S210					
S405		119	269	0.325	
S410					

ANALYSIS

Analytical Model

An attempt was made to simulate observed interaction of two lateral deformation by the analytical model assuming the flow rule. The model is the one developed by extending Degrading Tri-Linear model (Fig.12), which represents the hysteresis of flexural columns for one direction, to two directions through the plasticity (Takizawa and Aoyama, 1976; Yoshimura *et al.*, 1980). In the model, two surfaces representing crack criterion and yield criterion are assumed in the PX-PY plane, and according to the current state of PX and PY, the following three ranges are considered : ① elastic range, ② crack range and ③ yield range. The flow rule is used in the ranges of ② and ③. Fig.13 demonstrates changes of the range and direction of the normal to the surface when the specimens are loaded to the X direction.

Structural properties for one direction assumed in the analysis are listed in Table 2, where initial stiffness (K_0), crack load (P_c), yield load (P_y) and yield point secant stiffness reduction ratio (α_y) were computed using

conventional equations, and post-yield stiffness (p) was assumed as $K_o/1000$. The $P-\delta$ effect was considered also in the analysis.

Analytical Results

Computed lateral load vs. deformation relation is shown in Fig.3 by a dotted line. Except that the strength deterioration at large DX in the case of high axial load was not simulated, which was due to the post-yield stiffness being assumed positive ($K_o/1000$), the analysis reproduced the overall test results.

DX vs. DY relation and PX vs. DY relation are shown in Figs.4 and 5. The analysis could reproduce the following observations: ① DY was increasing as the loading proceeded, ② the rate of DY's increase was larger for greater PY_o and close for different axial loads, and ③ DY increased substantially when DX was large during the loading (Fig.4), in other words, near PX at the yield point (Fig.5). On the other hand, there was found a difference that the computed DY was smaller than the observed one at large DX in the case of high axial load. The reason of such difference is explained by the flow rule as shown in Fig.14: in the tests, the reduction of the yield surface accompanying the strength deterioration led to the direction of the normal to the yield surface being more inclined to the Y direction, while this was not considered in the analysis.

DX vs. DY relation and DX vs. DI ratio relation are shown in Fig.6.b for the third cycle. Symbol ▼ in the figure denotes the point where the load point reached the yield surface. DY increased near this point, and the DI ratio after this point ranged from 0.4 to 0.6 for S210 and S410 and was about 0.2 for S205 and S405, which in general coincided with the observations.

These results clearly indicate that the model assuming the flow rule well simulates the observed interaction of two lateral deformation, except for the region with strength deterioration. To cover this region, it is necessary to use the model like the one (Takizawa, 1977) incorporating the reduction of the yield surface.

CONCLUSION

The tests intended to observe deformation interaction of RC columns subjected to two-dimensional lateral loading were done, and applicability of the flow rule to RC columns was mainly discussed. The Flow rule proved to apply to RC columns for the interaction of two lateral deformation and also for lateral and axial deformation on some condition. In fact, the analytical model assuming this rule fairly well simulated the observed interaction of two lateral deformation.

REFERENCES

- Sato, Y., M. Yoshimura and K. Tsumura (1994). Displacement response of R/C columns subjected to bi-axial lateral loads. *Proceedings of the Japan Concrete Institute*, **16-2**, 653-658.
- Takizawa, H. and H. Aoyama (1976). Biaxial effects in modelling earthquake response of R/C structures. *Earthquake Engineering and Structural Dynamics*, John Wiley and Sons, Chichester, Sussex, England, **4-6**, 523-552.
- Takizawa, H. (1977). Biaxial and gravity effects in modeling strong-motion response of R/C structures. *Proceedings of the Sixth World Conference on Earthquake Engineering*, New Delhi, India, **2**, 1022-1027
- Tsumura, K., K. Saito, M. Yoshimura and H. Tsukagoshi (1994). Tests on columns with outer precast shell subjected to uni-axial and bi-axial lateral loads. *Proceedings of the Japan Concrete Institute*, **16-2**, 769-774.
- Yoshimura, M., H. Aoyama and M. Kawamura (1980). Analysis of reinforced concrete structure subjected to two-dimensional forces, part 1 : Analysis of RC columns subjected to bi-axial bending. *Transactions of the Architectural Institute of Japan*, **298**, 31-41